NUMERICAL INVESTIGATION ON SATURATED BOILING FLOW AND HEAT TRANSFER OF MIXTURE REFRIGERANT IN A VERTICAL RECTANGULAR MINI-CHANNEL

by

Jie CHEN [a], Weihua CAI [b*], Shulei LI [b], Yan REN [c], Hongqiang MA [d], and Yiqiang JIANG [c*]

[a] CNOOC Gas and Power Group, Beijing, China
[b] School of Energy Science and Engineering, Harbin Institute of Technology, Harbin, China
[c] School of Architecture, Harbin Institute of Technology, Harbin, China
[d] School of Civil Engineering, Lanzhou University of Technology, Lanzhou, China

Original scientific paper
https://doi.org/10.2298/TSCI171026046C

Plate-fin heat exchanger with rectangular minichannels, as a type of high-performance compact heat exchangers, has been widely used in liquefied natural gas field. However, the studies on saturated boiling flow and heat transfer for mixture refrigerant in plate-fin heat exchanger have been scarcely explored, which are helpful for designing more effective plate-fin heat exchanger using in liquefied natural gas field. Therefore, in this paper, the characteristics of saturated boiling flow and heat transfer for mixture refrigerant in rectangular minichannels of plate-fin heat exchanger were studied numerally based on validated model. Then, the effect of different parameters (vapor quality, mass flux, and heat flux) on heat transfer coefficient and frictional pressure drop were discussed. The results indicated that the boiling heat transfer coefficient and pressure drop are mainly influenced by quality and mass flux while heat flux has little influence on them. This is due to the fact that the main boiling mechanisms were forced convective boiling and the evaporation of dispersed liquid phase while nucleate boiling is slight.

Key words: *mini-channel, mixture refrigerant, saturated boiling, numerical simulation, CFX*

Introduction

Recently, much attention has been paid to plate-fin heat exchanger (PFHE), owing to its advantages, such as smaller size, more effective and so on. The PFHE with rectangular minichannels (gap size about 0.5-10 mm) [1], have been widely used in liquefied natural gas (LNG) field [2]. In PFHE, the main phenomenon in rectangular minichannels is saturated boiling flow and heat transfer (SBFHT) of mixture refrigerant. Therefore, better understanding of this phenomenon is benefit for the design and optimization of LNG PFHE. Due to the limitations of experimental measurements and computational technology, the realistic phenomenon has been scarcely studied until now.

Many experiments have been implemented to investigate the characteristics of SBFHT in minichannels [3, 4], most of which were focused on single-component refrigerant

*Corresponding authors, e-mail: caiwh@hit.edu.cn, jyq7245@sina.com

flow. According to some references [5, 6], the results showed that: a minichannel, unlike a tube (or macrochannel) with large diameter, has boiling heat transfer coefficient mainly depending on heat flux and system pressure, and not depending on vapor quality and mass flux. The studies suggested that in minichannels, the key mechanism for SBFHT was nucleate boiling and forced convective boiling could be ignored. But, other studies [7, 8] suggested that the contribution of nucleate boiling was remarkably slight. Besides, the studies proposed by Xu *et al*. [9] and Chien *et al*. [10] indacated that both the nucleate boiling and forced convective should be taken into account for SBFHT in minichannels. Feldman *et al*. [11] found that in minichannel flow, there existed two main mechanisms for SBFHT: nucleate boiling (*i. e*., boiling heat transfer coefficient depends on heat flux, but does not depend on vapor quality) and forced convection boiling (*i. e*., boiling heat transfer coefficient depends on vapor quality, and not independent of heat flux). Kew and Cornwell [12] also investigated SBFHT on a compact multi-channel plate. The results showed that there might exist one of four mechanisms in a narrow mini-channel: (a) nucleate boiling, (b) confined bubble boiling, (c) convective boiling, and (d) partial dry out. Balakrishnan *et al*. [13] researched SBFHT of R-134a/R-290/R-600a mixture in a smooth horizontal tube and found that the effect of nucleate boiling prevailing even at high vapor quality in a low mass and heat flux. Anwar *et al*. [14] studied the boiling heat transfer and pressure drop characteristics for R1234yf upward flow in a vertical minichannel with 1.60 mm diameter. The results showed that boiling heat transfer was strongly influenced by heat flux and saturation temperature, but showed insignificant dependence on mass flux and vapor quality. Meanwhile, the frictional pressure drop increased as mass flux and vapor quality increased while decreased with the increasing saturation temperature. Li *et al*. [15] also investigated the upward flow boiling for R1234yf and found that partial dry-out plays an important role in the heat transfer performance in minichannels. Boudouh *et al*. [16] carried out an experimental investigation on convective boiling heat transfer for water in minichannels. The results indicated that boiling heat transfer coefficients were typically much larger than those in convection processes involving a single phase. Actually, many experimental studies have investigated the behavior of SBFHT in minichannels, but there still exist a lack of information and reliable experimental data for engineering design. Meanwhile, there are many contradictions in the available literatures on this topic also, the characteristics of SBFHT on mixture refrigerant are less investigated in minichannels of LNG PFHE.

As the development of CFD, numerical simulation techniques have been widely used to investigate heat transfer [17, 18]. The simulations on multi-phase flow have been paid much attention owing to its wide appearance in engineering field. There are a few investigations on SBFHT in minichannels based on numerical simulations compared to the experimental studies [19, 20], but most investigations mainly focused on SBFHT in microchannels. Even though the simulation studies have increased regarding SBFHT in minichannels and microchannels, there still exist some important topics to be investigated. The mechanism that dominates SBFHT is still not clear. Also, there are a lack of accurate models to describe SBFHT in minichannels because the flow and heat transfer in minichannels and microchannels (the effect of surface tension) are entirely different from those in macrochannels [21, 22].

In this paper, a numerical model [23, 24], which includes an estimation method of diameter of dispersed phase, similarly with prediction method for interfacial length between the two phase proposed by Li *et al*. [25], to simulate SBFHT for mixture refrigerant in a vertical rectangular minichannel of LNG PFHE was introduced. Then, the influences of vapor quality, mass flux and heat flux on heat transfer coefficient and frictional pressure drop were also discussed. Finally, some important conclusions were drawn.

Mathematic-physical model

In this study, SBFHT process was simulated numerically for upward flow of mixture refrigerant in a vertical rectangular minichannel of LNG PFHE. Its cross-section dimension is a $b = 1.6$ 6.3 mm and the length is $l = 200$ mm, as shown in fig. 1.

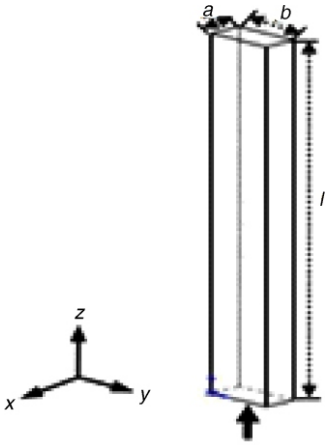

Figure 1. The computational model

Governing equations

In order to simulate multi-phase flow accompanying the thermal phase change, it used the inhomogeneous two-fluid model and thermal phase change model in this paper. Also, the Reynolds-averaged governing equations for conservation of mass, momentum and energy and turbulent quantities in a Cartesian co-ordinate system can be expressed as follows [23, 24].

Mass conservation

$$\frac{\partial}{\partial t}(r_v \rho_v) \quad (r_v \rho_v \mathbf{U}_v) \quad \Gamma_{vl} \tag{1}$$

$$\frac{\partial}{\partial t}(r_l \rho_l) \quad (r_l \rho_l \mathbf{U}_l) \quad \Gamma_{lv} \tag{2}$$

In eqs. (1) and (2), Γ_{vl} Γ_{lv}. The term Γ_{vl} 0 represents positive mass flow rate in per unit volume from liquid phase to vapor phase and Γ_{vl} can be expressed:

$$\Gamma_{vl} \quad \dot{m}_{vl} A_{vl} \tag{3}$$

where $\dot{m}_{vl}$ $\dot{m}_{lv}$.

The volume fraction of vapor (mixture refrigerant) is much more than that of liquid at high vapor quality so as to form a continuous region, but liquid phase shows discrete state. Therefore, liquid phase and vapor phase are considered as dispersed phase and vapor phase in this study. The interfacial area density A_{vl}, can be expressed:

$$A_{vl} \quad \frac{6 r_l}{d_l} \tag{4}$$

From eqs. (3) and (4), it is clearly seen that Γ_{vl} and Γ_{lv} in eqs. (1) and (2) are closely related to d_l and mass flow rate in per unit interfacial area.

Momentum conservation

$$\frac{\partial}{\partial t}(r_v \rho_v \mathbf{U}_v) \quad [r_v(\rho_v \mathbf{U}_v \quad \mathbf{U}_v)$$
$$\{r_v[\mu_v \quad \mu_{tv}][\mathbf{U}_v \quad (\mathbf{U}_v)^T]\} \quad r_v \quad p_v' \quad r_v(\rho_v \quad \rho_{\text{ref}})\text{g} \quad M_v \tag{5}$$

$$\frac{\partial}{\partial t}(r_l \rho_l \mathbf{U}_l) \quad [r_l(\rho_l \mathbf{U}_l \quad \mathbf{U}_l)$$
$$\{r_l[\mu_l \quad \mu_{tl}][\mathbf{U}_l \quad (\mathbf{U}_l)^T]\} \quad r_l \quad p_l' \quad r_l(\rho_l \quad \rho_{\text{ref}})\text{g} \quad M_l \tag{6}$$

Here the pressure constraint $p_v = p_l = p$ is given considering the same pressure field shared by all phases.

According to the discussion in references [23, 24], the standard k-ε model and zero equation model were chosen for vapor phase and liquid phase, respectively.

For vapor phase, turbulent viscosity can be modeled:

$$\mu_{tv} \quad C_\mu \rho_v \frac{k_v^2}{\varepsilon_v} \tag{7}$$

The transport equations of k and ε for vapor phase are shown:

$$\frac{\partial}{\partial t}(r_v \rho_v k_v) \quad r_v \ \rho_v \mathbf{U}_v k_v \quad \mu_v \quad \frac{\mu_{tv}}{\sigma_k} \quad k_v \quad r_v (P_{kv} \quad \rho_v \varepsilon_v) \tag{8}$$

$$\frac{\partial}{\partial t}(r_v \rho_v \varepsilon_v) \quad r_v \ \rho_v \mathbf{U}_v \varepsilon_v \quad \mu_v \quad \frac{\mu_{tv}}{\sigma_\varepsilon} \quad \varepsilon_v \quad r_v \frac{\varepsilon_v}{k_v}(C_{\varepsilon 1} P_{kv} \quad C_{\varepsilon 2} \rho_v \varepsilon_v) \tag{9}$$

where P_{kv} can be expressed:

$$P_{kv} \quad \mu_{tv} \ \mathbf{U}_v (\ \mathbf{U}_v \quad \mathbf{U}_v^T) \ \frac{2}{3} \ \mathbf{U}_v (3\mu_{tv} \ \mathbf{U}_v \quad \rho_v k_v) \quad P_{kbv} \tag{10}$$

where P_{kbv} can be modeled:

$$P_{kbv} \quad \frac{\mu_{tv}}{\mathrm{Pr}_{tv}} \mathrm{g} \ \rho_a \tag{11}$$

For liquid phase, turbulent viscosity, μ_{tl}, can be modeled:

$$\mu_{tl} \quad \rho_l f_\mu \mathbf{U}_{tl} l_{tl} \tag{12}$$

The length scale, l_{tl}, can be derived, shown:

$$l_{tl} \quad (V_D^{1/3})^{1/7} \tag{13}$$

Energy conservation

$$\frac{\partial}{\partial t}(r_v \rho_v H_v) \quad (r_v \rho_v \mathbf{U}_v H_v) \quad (r_v \lambda_v \ T_v) \quad Q_v \quad \Gamma_{vl} H_{vs} \tag{14}$$

$$\frac{\partial}{\partial t}(r_l \rho_l H_l) \quad (r_l \rho_l \mathbf{U}_l H_l) \quad (r_l \lambda_l \ T_l) \quad Q_l \quad \Gamma_{lv} H_{ls} \tag{15}$$

where $\Gamma_{vl} H_{vs}$ means heat transfer induced by interphase mass transfer into vapor phase and $\Gamma_{lv} H_{ls}$ represents interfacial values of enthalpy carried into liquid phase. So, their relation can be expressed as follows based on the thermal phase change model:

$$Q_v \quad Q_l \quad (\Gamma_{vl} H_{vs} \quad \Gamma_{lv} H_{ls}) \tag{16}$$

From eq. (16), it is clearly seen that the total heat transfer induced by interphase mass transfer equals to the total interphase sensible heat transfer. So to substitute eq. (3) into eq. (16), the expression for $\dot{m}_{vl}$ can be obtained:

$$\dot{m}_{vl} \quad \frac{Q_v \quad Q_l}{A_{vl}(H_{ls} \quad H_{vs})} \tag{17}$$

Based on the two resistance model, the sensible heat transfer process can be achieved using two heat transfer coefficients, which is defined on each side of the phase interface. So, Q_l and Q_v are expressed:

$$Q_l \quad h_l A_{vl}(T_s \quad T_l) \tag{18}$$

$$Q_v \quad h_v A_{vl}(T_s \quad T_v) \tag{19}$$

where T_s is determined from thermodynamic equilibrium. If the effect of surface tension on pressure is ignored, the interfacial temperature is considered:

$$T_s \quad T_{sat} \tag{20}$$

When considering liquid phase on one side of phase interface, a zero-resistance condition is used. That is to say, it assumes an infinite heat transfer coefficient in liquid phase side of phase interface, *i. e.*, $h_l = \infty$. This effect means to assume the interfacial temperature equal to that of liquid phase, $T_s = T_l$. Therefore, for vapor phase, h_v can be depicted:

$$h_v \quad \frac{\lambda_v \mathrm{Nu}_v}{d_l} \tag{21}$$

where Nu_v can be calculated based on Ranz-Marshall correlation [26], written:

$$\mathrm{Nu}_v \quad 2 \quad 0.6\,\mathrm{Re}_{vl}^{0.5}\,\mathrm{Pr}_{vl}^{0.3}, \quad 0 \quad \mathrm{Re}_{vl} \quad 200, \quad 0 \quad \mathrm{Pr}_{vl} \quad 250 \tag{22}$$

where Re_{vl} and Pr_{vl} are defined:

$$\frac{\mathrm{Re}_{vl} \quad \rho_v \left|\mathbf{U}_l \quad \mathbf{U}_v\right| d_l}{\mu_v}, \mathrm{Pr}_{vl} \quad \frac{\mu_v C_{pv}}{\lambda_v} \tag{23}$$

From eq. (4) and eqs. (18)-(22), it is clearly seen that d_l remarkably affects Q_l and Q_v. Meanwhile, from the previous analysis, it is found that d_l determines the simulation accuracy on SBHFT. However, in ANSYS CFX, d_l is always set as the constant value, which is not reasonable remarkably. Based on energy conservation, we have proposed an estimation method [23, 24] to calculate d_l based on energy conservation, which can be expressed:

$$d_l \quad \sqrt{\frac{3\bar{r}_l \lambda_v \mathrm{Nu}_v (1 \quad \gamma) l}{m x_{out} C_{pv}}} \tag{24}$$

According to eq. (24), it is clearly shown that d_l is determined based on the physical parameters (such as mixture density, specific heat, and thermal conductivity of vapor phase), Nusselt number on the vapor phase side of phase interface, vaporization rate, vapor quality at outlet, mass flux, and volume fraction of liquid. Nusselt number on vapor phase side of phase interface is estimated according to [26]. And the vaporization rate is also a key parameter to determine d_l.

Numerical schemes

In this paper, ANSYS CFX was used to simulate SBFHT of mixture refrigerant in a vertical rectangular minichannel of LNG PFHE. In order to check the influence of mesh amount on the simulation results, we chose three different meshes: 621000, 1290000, and 2130000 cells. The results showed that when the mesh amount exceeds 1290000 cells, the simulation results do not depend on the mesh amount. Therefore, to consider the computation efficiency, we chose 1.290,000 cells to simulate all cases in this paper. The Reynolds-averaged Navier-Stokes equations were used. The transient term, convection term and diffusion term were discretized, respectively, using the high resolution scheme (second-order accurate), the first-order backward Euler scheme and the central deferential scheme. The inhomogeneous two-fluid model was used. For boundary conditions: (1) at inlet, mass-flow, vapor volume fraction, and temperature were set, (2) at outlet, static pressure was set, and (3) at walls, constant heat flux was set. In order to ensure the simulation convergence, the steady-state solution was obtained firstly, and then the steady-state solution was used as the initial condition for simulating unsteady flows.

Mixture refrigerant

Mixture refrigerant consists of methane (mole fraction 42.06%), ethylene (36.12%), and propane (21.82%). In the simulation, mixture refrigerant was seemed as a simple substance, whose physical characteristic was calculated based on the different pressure and temperatures from RefProp 7 software. In the simulation, the pressure was kept at 0.315 MPa and the temperature was changed from 150 to 222 K so as to control the vapor quality. For each simulation case, the physical property of mixture refrigerant was constant since the temperature changed slightly at a given condition in a minichannel.

Results and discussion

From previous investigations it is aware that d_l remarkably influences the simulation accuracy, it is found that d_l remarkably influences the simulation accuracy. In our previous study [23, 24], we used eq. (24) to compute d_l in ANSYS CFX so as to simulate R21 upward flow in a vertical rectangular minichannel. The simulation results agreed well with experimental data from [2] when the vaporization rate equaled to 0.97 while the deviation between simulation results and experimental ones was within 15%, as shown in fig. 2. It was suggested that the expression for d_l is reasonable. So in this paper, we also adopted the same method to simulate SBFHT of mixture refrigerant in a vertical minichannel. This flow can remarkably influence the heat transfer coefficient and frictional pressure drop of LNG PFHE. Therefore, it is necessary to investigate SBFHT of mixture refrigerant considering the effect of vapor quality, mass flux and heat flux.

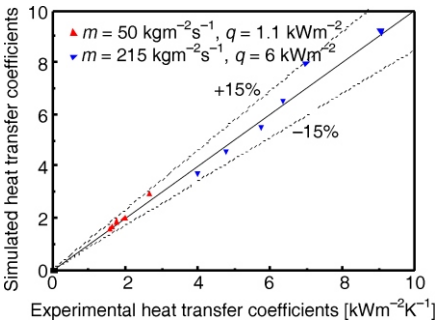

Figure 2. Comparison between simulation results and experiment ones [24, 25]

Flow pattern

When the pressure is kept at 0.315 MPa and the vapor quality is more than 0.3, the void fraction for the mixture refrigerant is always more than 0.98, in other word, the vapor phase almost fills the whole minichannel. Therefore, only the mist flow is observed in this study, as shown in fig.

3. It gives out the void fraction at outlet as $m = 200$ kg/m^{2}s, $x =$ $= 0.712$ and $q = 20$ kW/m^2. The result indicates that for the mist flow, vapor phase and liquid phase, evenly distributed in the minichannel except near the wall.

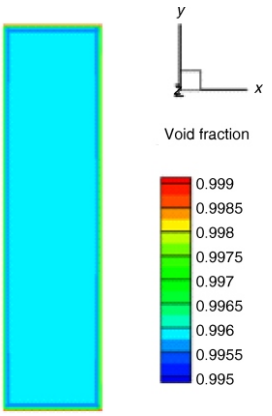

Figure 3. The typical flow pattern in this study

Heat transfer coefficient

Figures 4 and 5 show the heat transfer coefficient as a function of vapor quality at different mass fluxes with heat flux $q = 20$ kW/m^2 and at different heat fluxes with mass flux $m = 250$ kg/m^{2}s, respectively. From figs. 4 and 5, it is found that the heat transfer coefficient remarkably increases with the increasing vapor quality. From this point, it proves that forced convection boiling plays an important role in SBFHT of mixture refrigerant. Compared to the results at low vapor quality, the heat transfer coefficient shows more quickly increase at high vapor quality. It means that the evaporation of dispersed liquid phase is the heat transfer mechanism at high vapor quality. Meanwhile, the effect of mass flux is more obvious at high vapor quality. The heat transfer coefficient is slightly influenced by heat flux at different vapor qualities. That is to say, the contribution of nucleation boiling can be ignored for heat transfer in the saturated boiling heat transfer process of mixture refrigerant in vertical rectangular minichannels of LNG PFHE.

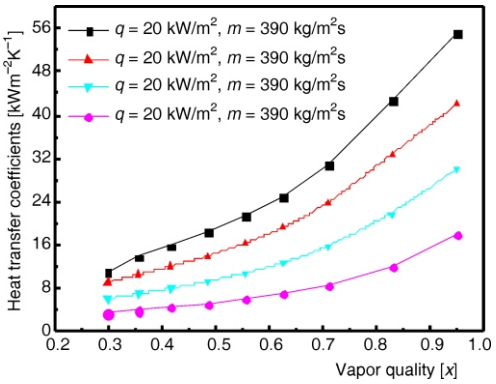

Figure 4. Heat transfer coefficients *vs.* vapor quality at different mass fluxes

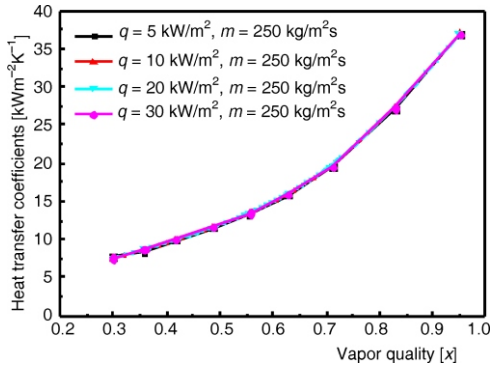

Figure 5. Heat transfer coefficient *vs.* vapor quality at different heat fluxes

Figures 6 and 7 show the relation between heat transfer coefficient and mass flux at different vapor qualities with heat flux $q = 20$ kW/m^2 and at different heat fluxes with vapor quality $x = 0.627$, respectively. It is found that the heat transfer coefficient can be remarkably affected by mass flux and also linearly increases with the increasing mass flux. In addition, fig. 6 also indicates that the heat transfer coefficient increases more quickly with mass flux at high vapor quality and the effect of vapor quality is more obvious at high mass flux. This is due to the fact that the boiling mechanism of forced convection enhances with the increase of mass flux and vapor quality in the saturated boiling heat transfer process of mixture refrigerant. Meanwhile, at different mass fluxes, the effect of heat flux can be ignored for heat transfer coefficient.

Frictional pressure drop

Figures 8 and 9 present the relationship between frictional pressure drop and vapor quality at different mass fluxes with heat flux $q = 20$ kW/m^2 and at different heat fluxes with mass flux $m = 250$ kg/m^{2}s, respectively. The frictional pressure drop is obviously influenced by vapor quality

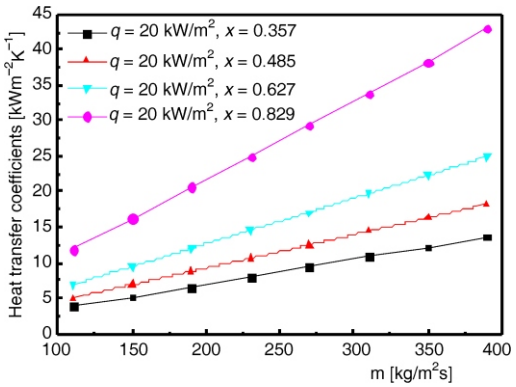

Figure 6. Heat transfer coefficient *vs.* mass flux at different vapor qualities

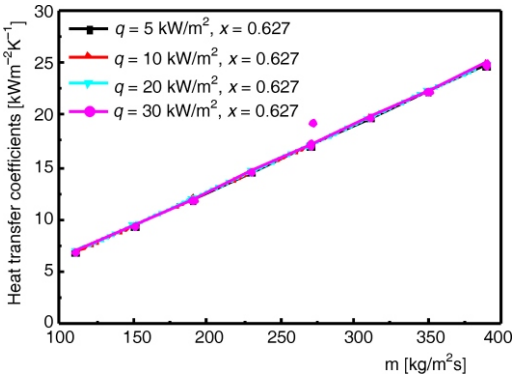

Figure 7. Heat transfer coefficient *vs.* mass flux at different heat fluxes

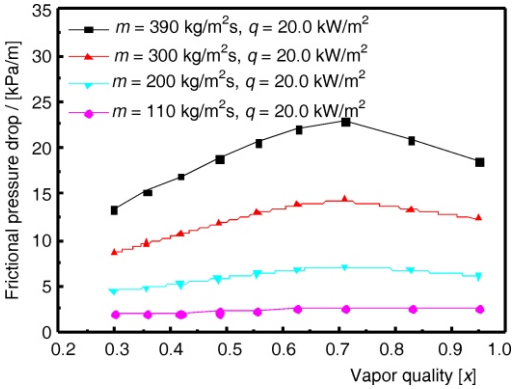

Figure 8. Frictional pressure drop *vs.* vapor quality at different mass fluxes

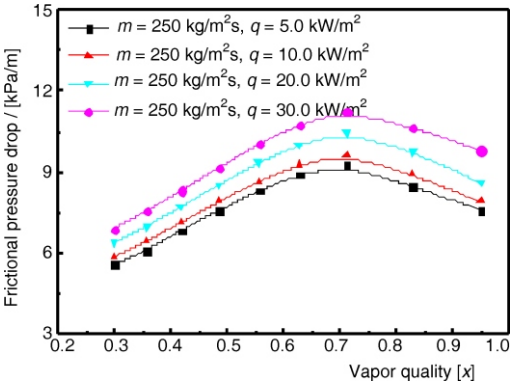

Figure 9. Frictional pressure drop *vs.* vapor quality at different heat fluxes

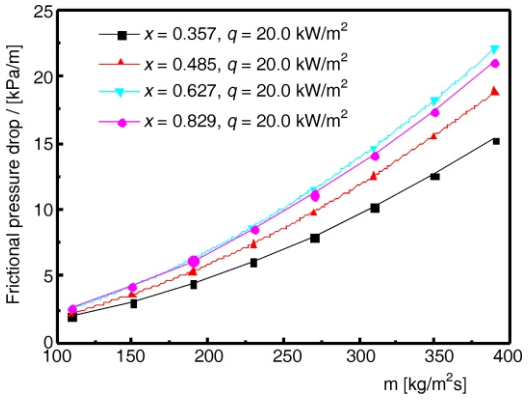

Figure 10. Frictional pressure drop *vs.* mass flux at different vapor qualities

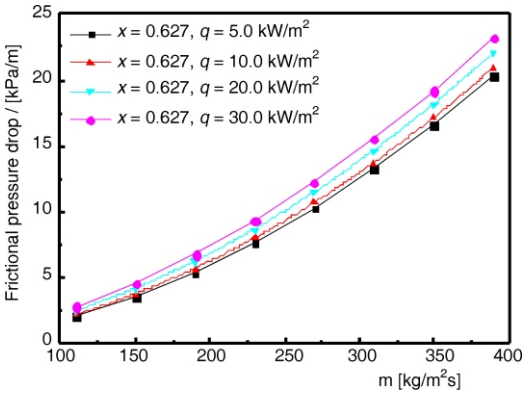

Figure 11. Frictional pressure drop *vs.* mass flux at different heat fluxes

when mass flux is more than 200 kg/m^{2}s. At the same time, the frictional pressure drop increases with the increasing vapor quality when the vapor quality is not more than 0.7. But the frictional pres-

sure drop decreases as vapor quality increases when the vapor quality is more than 0.7. Besides, the effect of mass flux is obvious for the frictional pressure drop. The larger mass flux is, the higher frictional pressure drop is. Figure 9 also shows that the frictional pressure drop is obviously influenced by heat flux and increase with the increase of heat flux. In other words, the frictional pressure drop reaches a peak value at vapor quality $x = 0.7$. The frictional pressure drop increases as the vapor quality increases when the vapor quality is less than 0.7.

Figures 10 and 11 show frictional pressure drop as a function of mass flux at different vapor qualities with heat flux $q = 20$ kW/m^2 and at different heat fluxes with vapor quality $x = 0.627$. The frictional pressure drop is remarkably affected by mass flux and increases with the increasing mass flux. The frictional pressure drop shows more quick increase with mass flux at high mass flux and the effect of vapor quality is more remarkable at high mass flux. Meanwhile, the effect of heat flux is also remarkable for the frictional pressure drop at the different mass fluxes in the SBFHT process of mixture refrigerant in vertical rectangular minichannels of LNG PFHE.

Conclusions

In this paper, a computational model was introduced to simulate SBFHT of mixture refrigerant at high vapor quality ($x = 0.3$~0.95) in a vertical rectangular minichannel of LNG PFHE. The characteristics and mechanism of SBFHT were analyzed. Some important conclusions can be drawn as follows.

The heat transfer coefficient remarkably increases with the increase of vapor quality and mass flux, but almost does not change with heat flux.

The frictional pressure drop obviously increases with the increasing mass flux and slightly increases with the increase of heat flux while as the vapor quality increases, the frictional pressure drop firstly increases and then decreases with a peak value at vapor quality $x = 0.7$.

For SBFHT at high vapor quality, forced convection boiling and the evaporation of dispersed liquid phase are the main heat transfer mechanism while nucleate boiling can be ignored.

Acknowledgment

The authors are grateful for the support of the research funds from 863 program on National High Technology Research and Development Program (2013AA09A216) and postdoctoral scientific research developmental fund of Heilongjiang Province (LBH-Q15043).

Nomenclature

A_{vl} – interfacial area density between liquid phase and vapor phase
C_{pv} – specific heat at constant pressure, [Jkg^{-1}K^{-1}]
C_μ – a constant, (= 0.09)
$C_{\varepsilon 1}$ – constant with the value of 1.44
$C_{\varepsilon 2}$ – constant with the value of 1.92
d_l – mean diameter of dispersed phase, [m]
f_μ – a proportionality constant
g – gravity, [ms$_{-2}$]
H – enthalpy, [Jkg^{-1}]
H_{ls} – interfacial values of enthalpy carried into liquid phase
H_{vs} – interfacial values of enthalpy carried into vapor phase
h_l – heat transfer coefficient for liquid phase on one side of phase interface
h_v – heat transfer coefficient for vapor phase on one side of phase interface
k – turbulent kinetic energy
l_t – turbulence length scale, [m]
M – the sum of interfacial forces acting on a phase due to the presence of other phases
m – mass-flux, [kgm^{-2}s^{-1}]
$\dot{m}_{vl}$ – mass-flow rate in per unit interfacial area from liquid phase to vapor phase
Nu_v – Nusselt number for vapor phase side of phase interface
P_{kbv} – buoyancy production term for vapor phase
p – pressure, [Pa]
q – heat flux, [Wm^{-2}]
Q_l – interphase sensible heat transfer to liquid phase across interfaces

Q_v – interphase sensible heat transfer to vapor phase across interfaces
q – heat flux, [Wm^{-2}]
Re_{vl} – Reynolds number of vapor phase
r – volume fraction
T – temperature, [K]
t – time, [s]
U – velocity, [ms^{-1}]
U_t – turbulent velocity scale, [ms^{-1}]
V_D – the fluid domain volume
x – vapor quality

Greek symbols

Γ_{lv} – mass-flow rate in per unit volume from vapor phase to liquid phase
Γ_{vl} – mass-flow rate in per unit volume from liquid phase to vapor phase
γ – vaporization rate
ε – turbulent dissipation rate
λ – thermal conductivity, [$Wm^{-1}K^{-1}$]
μ – viscosity, [Pa s]
μ_t – turbulent viscosity, [Pa s]
ρ – density, [kgm^3]
σ_k – constant with the value of 1.3
$_\varepsilon$ – constant with the value of 1.0

Other symbol

– tensor product

Subscripts

l – liquid phase
out – outlet
sat – saturation
s – interfacial
t – turbulence
v – vapor phase

References

[1] Jiang, W. C., *et al*., A Comparison of Brazed Residual Stress in Plate-fin Structure Made of Different Stainless Steel, *Materials & Design, 30* (2009), 1, pp. 23-27
[2] Kuznetsov, V. V., Shamirzaev, A. S., Boiling Heat Transfer for Freon R21 in Rectangular Minichannel, *Heat Transfer Engineering, 28* (2007), 8-9, pp. 738-745
[3] Kandlikar, S. G., Development of a Flow Boiling Map for Subcooled and Saturated Flow Boiling of Different Fluids inside Circular Tubes, *Journal of Heat Transfer-Transactions of the ASME, 113* (1991), 1, pp. 190-200
[4] Kandlikar, S. G., Balasubramanian, P., An Extension of the Flow Boiling Correlation to Transition, Laminar, and Deep Laminar Flows and Microchannels, *Proceedings*, Selected Papers Presented at the First International Conference on Microchannels and Minichannels, 3rd Taylor and Francis Ltd, Rochester Institute of Technology, Rochester, N. Y., USA, 2004, pp. 86-93
[5] Charnay, R., *et al*., Flow Boiling Heat Transfer in Minichannels at High Saturation Temperatures: Part – Experimental Investigation and Analysis of the Heat Transfer Mechanisms, *International Journal of Heat and Mass Transfer, 87* (2015), Aug., pp. 636-652
[6] Charnay, R., *et al*., Flow Boiling Heat Transfer in Minichannels at High Saturation Temperatures: Part I – Assessment of Predictive Methods and Impact of Flow Regimes, *International Journal of Heat and Mass Transfer, 87* (2015), Aug., pp. 653-672
[7] Oliveira, J. D., *et al*., An Experimental Investigation on Flow Boiling Heat Transfer of R-600a in a Horizontal Small Tube, *International Journal of Refrigeration, 72* (2016), Dec., pp. 97-110
[8] Marzoa, M. G., *et al.*, Experimental Flow Boiling Heat Transfer in a Small Polyimide Channel, *Applied Thermal Engineering, 103* (2016), June, pp. 1324-1338
[9] Xu, Y., *et al*., An Experimental Study of Flow Boiling Heat Transfer of R134a and Evaluation of Existing Correlations, *International Journal of Heat and Mass Transfer, 92* (2016), Jan., pp. 1143-1157
[10] Chien, N. B., *et al*., Boiling Heat Transfer of R32, CO_2 and R290 inside Horizontal Minichannel, *Energy Procedia, 105* (2017), May, pp. 4822-4827
[11] Feldman, A., *et al.*, Nucleate and Convective Boiling in Plate Fin Heat Exchangers, *International Journal of Heat and Mass Transfer, 43* (2000), 18, pp. 3433-3442
[12] Kew, P. A., Cornwell, K., Correlations for the Prediction of Boiling Heat Transfer in Small-Diameter Channels, *Applied Thermal Engineering, 17* (1997), 8-10, pp. 705-715
[13] Balakrishnan, R., *et al*., Flow Boiling Heat Transfer Coefficient of R-134a/R-290/R-600a Mixture in a Smooth Horizontal Tube, *Thermal Science, 12* (2008), 3, pp. 33-44
[14] Anwar, Z., *et al*., Flow Boiling Heat Transfer, Pressure Drop and Dryout Characteristics of R1234yf: Experimental Results and Predictions, *Experimental Thermal and Fluid Science, 66* (2015), Sept., pp. 137-149

[15] Li, J., *et al*., Up-Flow Boiling of R1234yf in Aluminum Multi-Port Extruded Tubes, *International Journal of Heat and Mass Transfer, 114* (2017), Nov., pp. 826-836
[16] Boudouh, M., *et al*., Experimental Investigation of Convective Boiling in Mini-Channels: Cooling Application of the Proton Exchange Membrane Fuel Cells, *Thermal Science, 21* (2017), 1, pp. 223-232
[17] Dong, Z., *et al.*, Numerical Study of Vapor Bubble Effect on Flow and Heat Transfer in Microchannel, *International Journal of Thermal Sciences, 54* (2012), Apr., pp. 22-32
[18] Magnini, M., *et al.*, Numerical investigation of Hydrodynamics and Heat Transfer of Elongated Bubbles during Flow Boiling in a Microchannel, *International Journal of Heat and Mass Transfer, 59* (2013), Apr., pp. 451-471
[19] Krishnan, R. N., *et al*., Performance of Numerical Schemes in the Simulation of Two-Phase Free Flows and Wall Bounded Minichannel Flows, *Chemical Engineering Science, 65* (2010), 18, pp. 5117-5136
[20] Son, G., *et al*., Numerical Simulation of Bubble Merger Process on a Single Nucleation Site during Pool Nucleate Boiling, *Journal of Heat Transfer, 124* (2002), 1, pp. 51-62
[21] Kandlikar, S. G., Fundamental Issues Related to Flow Boiling in Minichannels and Microchannels, *Experimental Thermal and Fluid Science, 26* (2002), 2-4, pp. 389-407
[22] Zhang, W., *et al*., Correlation for Flow Boiling Heat Transfer in Mini-Channels, *International Journal of Heat and Mass Transfer, 47* (2004), 26, pp. 5749-5763
[23] Cai, W. H., *et al*., Numerical Investigation on Saturated Boiling Heat Transfer in a Vertical Rectangular Minichannel, *Proceedings*, ASME 2015 Joint Fluids Engineering Conference, Seoul, Korea, 2015, pp. V001T30A003
[24] Ma, H. Q., *et al*., Numverical Investigation on Saturated Boiling and Heat Transfer Correlations in a Vertical Rectangular Minichannel, *International Journal of Thermal Science, 102* (2016), Apr., pp. 285-299
[25] Li, S. L., *et al*., Numerical Study on the Flow and Heat Transfer Characteristics of Forced Convective Condensation with Propane in a Spiral Pipe, *International Journal of Heat and Mass Transfer, 117* (2018), Feb., pp. 1169-1187
[26] Ranz, W. E., Marshall, W. R., Evaporation from Drops, *Chemical Engineering Progress, 48* (1952), 3, pp. 141-146

Paper submitted: October 26, 2017
Paper revised: November 23, 2017
Paper accepted: November 23, 2017